

pubs.acs.org/NanoLett Letter

# Atomic Resolution Imaging of Highly Air-Sensitive Monolayer and Twisted-Bilayer WTe<sub>2</sub>

Fang Yuan, Yanyu Jia, Guangming Cheng, Ratnadwip Singha, Shiming Lei, Nan Yao, Sanfeng Wu,\* and Leslie M. Schoop\*



Cite This: Nano Lett. 2023, 23, 6868-6874



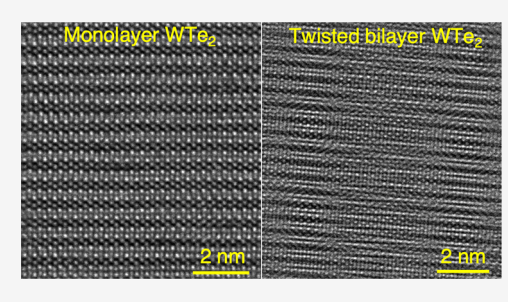
**ACCESS** I

III Metrics & More

Article Recommendations

Supporting Information

**ABSTRACT:** Bulk Td-WTe $_2$  is a semimetal, while its monolayer counterpart is a two-dimensional (2D) topological insulator. Recently, electronic transport resembling a Luttinger liquid state was found in twisted-bilayer WTe $_2$  (tWTe $_2$ ) with a twist angle of  $\sim$ 5°. Despite the strong interest in 2D WTe $_2$  systems, little experimental information is available about their intrinsic microstructure, leaving obstacles in modeling their physical properties. The monolayer, and consequently tWTe $_2$ , are highly air-sensitive, and therefore, probing their atomic structures is difficult. In this study, we develop a robust method for atomic-resolution visualization of monolayers and tWTe $_2$  obtained through mechanical exfoliation and fabrication. We confirm the high crystalline quality of mechanically exfoliated



WTe<sub>2</sub> samples and observe that tWTe<sub>2</sub> with twist angles of  $\sim$ 5 and  $\sim$ 2° retains its pristine moiré structure without substantial deformations or reconstructions. The results provide a structural foundation for future electronic modeling of monolayer and tWTe<sub>2</sub> moiré lattices.

**KEYWORDS:** moiré patterns, scanning transmission electron microscopy, atomic resolution imaging, monolayer WTe<sub>2</sub>, twisted bilayer WTe<sub>2</sub>, air-sensitive

The field of two-dimensional (2D) crystals and artificial structures is rapidly expanding and providing new opportunities in many areas of physics, chemistry, and engineering. The 2D material library is rich.<sup>1-3</sup> It has been suggested that more than 1000 layered crystals can potentially be exfoliated down to their monolayer limit,<sup>3</sup> only considering known layered 3D compounds. The physical properties of the majority of 2D crystals in this large class remain unexplored or poorly explored, especially those beyond the air-stable materials, such as graphene and semiconducting transitionmetal dichalcogenides (TMDs). In general, many 2D crystals and vdW structures are sensitive to their environment, though their bulk phases may or may not be stable in air. Hence, the investigation of 2D crystals requires careful processing to avoid degradation and contamination, which often calls for the development of new synthesis, fabrication, and measurement techniques.

An outstanding example is tungsten ditelluride (WTe<sub>2</sub>). Bulk WTe<sub>2</sub> exists in the Td phase, which belongs to the space group  $Pmn2_1$  and lacks inversion symmetry. When exfoliating into individual monolayers, the resulting symmetry elements switch to space group  $P2_1m$  with an inversion center. The monolayer of Td-WTe<sub>2</sub> is also sometimes referred to as the 1T' phase in the literature. Each isolated WTe<sub>2</sub> monolayer consists of one W plane sandwiched between two Te planes, where each W atom is bonded to six Te atoms, forming distorted-octahedral polyhedrons. Within the W plane, the W

atoms form zigzag chains along the a axis. Monolayer WTe2 was shown experimentally to be a good insulator and exhibit the QSH effect up to 100 K.5-7 It was the first realization of a QSH insulator in an isolated 2D monolayer device. The insulating ground state of the monolayer is surprising, as it was not captured by early predictions<sup>4</sup> and bulk WTe<sub>2</sub> is a semimetal.<sup>8,9</sup> Recent studies have further suggested that the insulating ground state stems from the formation of excitons: i.e., monolayer  $WTe_2$  is an excitonic insulator. Upon moderate electrostatic gating, the monolayer insulator can be further converted to a superconductor. 13,14 More recently, twisted-bilayer WTe2 (tWTe2) with a small interlayer twist angle (near 5°) was shown to exhibit a strongly anisotropic 2D phase that behaves like an array of 1D conducting channels described by the Luttinger liquid theory. 15 The result may lead to new advances in the field of correlated quantum matter and non-Fermi liquid. Independent scanning tunneling microscopic measurements on tWTe2 focused on how twisting tunes the QSH properties at various twist angles and found consistent moiré effects at small twist angles.1

**Received:** March 28, 2023 **Revised:** July 17, 2023 **Published:** July 21, 2023





#### **TEM Sample Preparation Process**

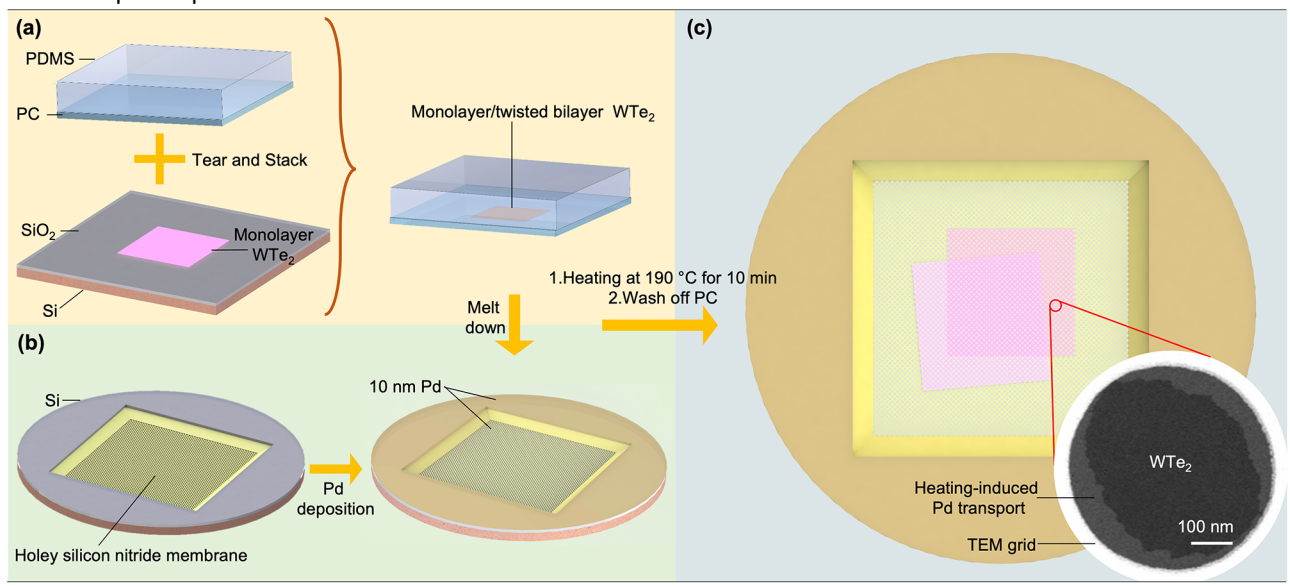


Figure 1. Schematic representation of the fabrication of monolayer and twisted-bilayer WTe<sub>2</sub> for plan-view TEM studies. (a) tWTe<sub>2</sub> is prepared by the "tear and stack" technique, using a polycarbonate (PC)/polydimethylsiloxane (PDMS) stamp. (b) 10 nm Pd is deposited on holey  $Si_3N_4$  TEM grids; subsequently, the sample is placed on the pretreated TEM grid by melting down the stamp. (c) Heating at 190 °C for 10 min causes some of the Pd to transport along the (t)WTe<sub>2</sub> layers. This causes the specimens to be strongly attached to the TEM grid; finally the PC residues are washed off with chloroform. Because of the enhanced adhesion due to the Pd transport on WTe<sub>2</sub>, the samples survive the washing step. The inset shows one enlarged TEM grid containing resulting freestanding WTe<sub>2</sub> samples.

Despite these exciting developments in probing the electronic properties of the 2D WTe2 system, direct experimental imaging of their atomic structures largely falls behind, mainly due to WTe2's air-sensitive nature. The issue is severe for understanding the physics of 2D WTe<sub>2</sub> systems since the underlying structures in realistic samples may well be different from the simulated patterns based on rigid monolayers. As a comparison, in the extensively studied twisted bilayer graphene (TBG) systems, it has been well established that atomic scale moiré reconstruction and strain effects are critical to its structural and electronic properties..<sup>17-21</sup> Lattice reconstruction has been discussed in airstable twisted-bilayer TMDs and TMD heterostructures as well.<sup>22-24</sup> In particular, scanning/transmission electron microscopy (S/TEM) is widely used as a direct structural visualization tool. 17,21-25 S/TEM studies have shown that atomic and electronic reconstructions in TBG are significant when the twist angle is smaller than 1°, resulting in a gradual transition from an incommensurate moiré structure to an array of commensurate domains. 17,21,25 In general, it is important to directly visualize, experimentally, the underlying 2D crystals and moiré structures of interest. As far as we know, only a few studies have imaged monolayer WTe2 thus far26-28 and no direct imaging of tWTe<sub>2</sub> samples with an atomic resolution exist. Beyond WTe2, challenges are universally presented for air-sensitive 2D materials and their moiré structures.

We first developed a step-by-step methodology to obtain atomic-resolution STEM images of the highly air-sensitive monolayer and tWTe<sub>2</sub>. Our study reveals that WTe<sub>2</sub> monolayers obtained through exfoliation with Scotch tape exhibit a flat morphology without notable rippling or atom vacancies. This observation stands in contrast to the CVD-grown samples that were previously investigated.<sup>27</sup> This highlights the differences in monolayer WTe<sub>2</sub> samples that are important to consider when discussing their physical

properties. We also verify that the in-plane structure of WTe<sub>2</sub> monolayers does not change in comparison to that of bulk crystals, which is an important observation for electronic modeling of the monolayer. We subsequently employ a methodology identical with that used to image tWTe<sub>2</sub>, derived from exfoliated monolayers. Our findings reveal that tWTe<sub>2</sub> with angles of  $\sim$ 5 and  $\sim$ 2° exhibit a strong resemblance to the anticipated moiré pattern, pointing to the absence of significant lattice reconstructions, although reconstructions might still appear at other angles. This information is important for understanding the intriguing electronic properties in the system, including Luttinger liquid physics. Herein, we demonstrate the first S/TEM study on a twisted-bilayer WTe2 with an orthorhombic lattice, and the techniques can be readily extended to directly visualize tWTe2 at arbitrary twist angles, as well as other air-sensitive 2D structures in the future.

WTe<sub>2</sub> crystals were prepared via self-flux growth. Studies of the residual-resistance ratio (RRR) and energy dispersive X-ray spectroscopy (EDS) confirmed the high quality of WTe2 crystals (Figures S1 and S2). Monolayers of WTe2 were exfoliated onto Si/SiO<sub>2</sub> wafers using Scotch tape (Figure S3). More experimental details are given in the Supporting Information (SI). The plan-view TEM sample preparation process is shown in Figure 1. Suspending 2D materials onto a holey TEM grid can be challenging due to the fragility of the materials and weak bonding between the materials and the grid. It is also important for the materials to survive the subsequent chemical cleaning processes. We initially tried to transfer WTe<sub>2</sub> specimens directly onto holey Si<sub>3</sub>N<sub>4</sub> TEM grids (both as-bought and O<sub>2</sub> plasma cleaned), but the atomically thin flake would usually not survive the chloroform bath necessary for removing the polymer layer, as the flake tends to move or break during the process. Although monolayers of WTe2 may still be found on a TEM grid this way, the uncontrolled motion makes it challenging to prepare twisted

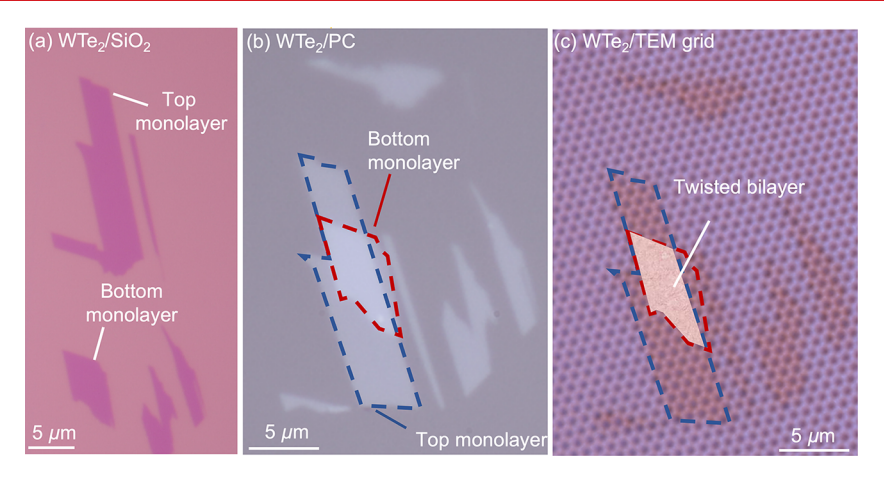


Figure 2. Optical microscopy (OM) images of monolayer and twisted-bilayer WTe<sub>2</sub>. (a) OM image of a monolayer WTe<sub>2</sub> on a SiO<sub>2</sub>/Si substrate. (b) OM image of a monolayer and a twisted-bilayer WTe<sub>2</sub> on a PC/PDMS stamp after "tear and stack". (c) OM image of a monolayer and a twisted-bilayer WTe<sub>2</sub> after transferring to a holey  $Si_3N_4$  TEM grid. The twisted-bilayer WTe<sub>2</sub> is highlighted by a pink shadow.

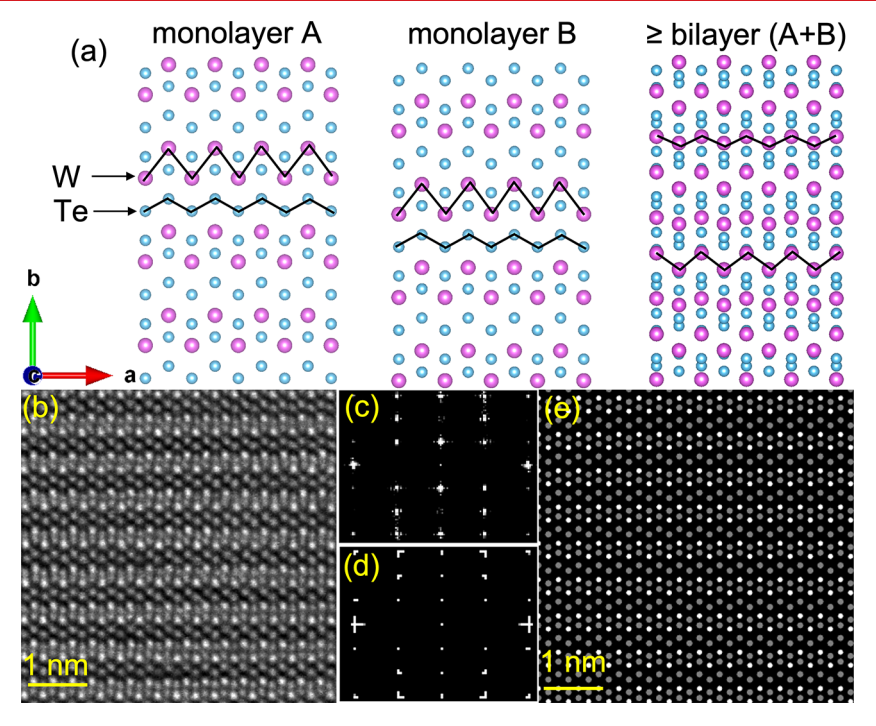


Figure 3. Experimental and simulated STEM imaging of monolayer WTe<sub>2</sub>, viewed along the *c* axis. (a) Crystal structure of single- and few-layer WTe<sub>2</sub>. Experimental (b, c) and simulated (d, e) HAADF-STEM images and FFT patterns for monolayer WTe<sub>2</sub>. Simulated electron diffraction patterns used the structural information from ref 30.

samples with fixed twist angles. Thus, an improved procedure was developed to increase the adhesion of WTe2 specimens on the TEM grid, as described in the following. To prepare the TEM grids, we first treated them with  $O_2$  plasma and subsequently deposited a 10 nm layer of Pd, which we found greatly increases the adhesion between WTe2 and the grid after heat treatment at 190 °C for 10 min, which causes some of the Pd to transport along the (t)WTe2 layers.29 Therefore, the specimens became strongly attached to the TEM grid. Using this specially treated adhesion-enhanced Si<sub>3</sub>N<sub>4</sub> TEM grids, suspended monolayer and tWTe<sub>2</sub> specimens could be reliably obtained. (Figure 2) More details on how to obtain clean and crystalline monolayer and tWTe2 samples can be found in the SI section Ensuring High-quality Specimens and Figure S4. This method could be an efficient route for preparing many other atomically thin TEM specimens, as well. The optimized adhesion layer to deposit on the TEM grid may vary depending on the material under investigation.

Although the primary objective of this study is to explore the intrinsic structure of monolayer and twisted-bilayer WTe<sub>2</sub> by using S/TEM, it is crucial to conduct a thorough characterization of the structure and composition of bulk WTe<sub>2</sub> crystals by using cross-sectional S/TEM. This characterization is necessary to ensure the exclusion of any inaccuracies arising from atomic-level impurities or defects. Our investigations have verified that our bulk WTe<sub>2</sub> crystals exhibit minimal defects and impurities, making them suitable for obtaining high-quality monolayer and twisted-bilayer WTe<sub>2</sub>. For more detailed information, including structural characterization and composition analysis of bulk *Td*-WTe<sub>2</sub> crystals, please refer to the SI section titled Structural Characterization and

Nano Letters pubs.acs.org/NanoLett Letter

Composition Analysis of Bulk Td-WTe2 Crystals and consult Figures S5 and S6 and Table S1.

We also took the opportunity to study the instability and degradation of free-standing monolayer WTe<sub>2</sub> upon air exposure, where we found that it transforms to a uniform amorphous oxide within 1/2 h; more discussion on the degradation of monolayer WTe<sub>2</sub> in ambient conditions can be found in the section Instability and Degradation of Single- and Few-Layer WTe<sub>2</sub> Nanosheets in Ambient Conditions and Figure S7 in the SI. For all other S/TEM images, samples were carefully preserved in Ar or under vacuum during the entire experimental procedure to prevent sample degradation.

We are now proceeding to analyze ultrathin WTe<sub>2</sub> samples using S/TEM. Previous S/TEM imaging of atomically thin WTe<sub>2</sub> was limited to 60–80 kV to reduce the electron beam damage.<sup>26–28</sup> In this work, we imaged monolayer WTe<sub>2</sub> and tWTe<sub>2</sub> under 300 kV to obtain atomic-resolution images for microstructural analysis. Experimental details about how we reduce beam damage can be found in the section Beam Damage: 80 kV vs 300 kV of the SI and Figure S8. We begin with discussing the images of monolayer WTe<sub>2</sub>, as these provide the foundation for understanding twisted samples, discussed later in the paper.

Figure 3 shows the crystal structures of single- and few-layer WTe<sub>2</sub> viewed along the c axis. There are significant differences between single- and few-layer WTe2: (i) the Te atoms in monolayer WTe2 form zigzag chains along the a axis, and such chain features disappear in few-layer samples due to the ABAB stacking order; (ii) the distribution of the W atoms along the a axis becomes more complex when more than one layer is considered, as visualized in Figure 3a. Since the image intensity/brightness is directly related to the square of the atomic Z number in HAADF-STEM images, we can identify W and Te atoms according to their brightness. This information is also useful to distinguish monolayer from few-layer samples. Figure 3b,e displayd the experimental and simulated atomicresolution HAADF-STEM images of a monolayer WTe2, while Figure 3c,d shows the corresponding FFT patterns. The experimental images display intact structures, which agree well with the expected results for a monolayer. No beam-induced lattice displacements or electron-induced vacancies are observed. These results confirm that monolayer WTe2 remains in the same structure as in its bulk *Td* orthorhombic phase. For comparison, an image of a few-layer flake is shown in Figure S9 in the SI; it agrees well with the structure of few layers in Figure 3a. Therefore, it is easy to distinguish monolayers from thicker flakes. Table 1 lists the d-spacing of bulk, exfoliated single-layer, and few-layer Td-WTe2. Within the measurement error range of TEM, we do not observe significant changes in d-spacing in the (200), (020), (120), and (130) lattice planes, when the thickness is decreased. Thus, the crystal structure of

Table 1. Experimental and Simulated d-Spacing of Bulk, Scotch-Tape Exfoliated Single-Layer, and Few-Layer Td-WTe<sub>2</sub>

	lattice plane			
	(200)	(020)	(120)	(130)
sim bulk <sup>30</sup> (Å)	1.74	3.14	2.34	1.80
exp few-layer (Å)	1.72	3.10	2.30	1.76
exp monolayer (Å)	1.73	3.16	2.31	1.78

the monolayer seems to undergo no significant change or relaxation as compared to its bulk form.

Another important consideration in characterizing monolayers is the potential presence of "rippling", which may introduce strain and impact the electronic properties. A recent study<sup>27</sup> reported significant rippling in CVD-grown monolayer WTe<sub>2</sub>. This raises the question of whether WTe<sub>2</sub> monolayers are inherently corrugated or if the observed rippling is a consequence of sample preparation. It has been demonstrated that high temperatures during the CVD process (up to 820 °C) can induce rippling in monolayer samples.<sup>31</sup>

In our study, the samples were exposed to a maximum temperature of 190 °C for 10 min, which is considerably lower than those reported in previous studies. This relatively lower temperature and shorter exposure time may have contributed to the flatter appearance of our samples. To further support this observation, we examined larger-scale monolayer WTe<sub>2</sub> in multiple locations (see Figure S10) and found no evidence of rippling in the investigated areas. However, it should be noted that additional research is needed to confirm whether the difference in heat exposure is indeed responsible for the flatter samples. Our findings suggest that perfectly flat monolayers of WTe<sub>2</sub> can be obtained and emphasize the importance of sample quality and preparation methods in studying their properties.

Having established that WTe $_2$  monolayers can be imaged at atomic resolution and are of high quality, we can now proceed to study the intrinsic structure of tWTe $_2$ , focusing on a  $\sim 5^\circ$  twist angle. At this angle, the recently observed exceptionally large transport anisotropy together with the power law scaling in conductance in tWTe $_2$  has implied the formation of a strongly correlated 2D non-Fermi liquid phase consisting of an array of 1D Luttinger liquids. <sup>15</sup> However, the atomic structure of this new moiré material remains unexplored.

Figure 4 shows an atomic-resolution STEM image of tWTe<sub>2</sub> with a twist angle of  $\sim 5^{\circ}$ . We confirm the twist angle to be  $\sim 5^{\circ}$ via the FFT pattern in the inset, which agrees with the targeted stack angle aimed at in the fabrication. Each monolayer WTe<sub>2</sub> contains sandwiched Te-W-Te layers (Figure S5a), and consequently, tWTe2 consists of six atomic layers. For better illustration, it helps to consider the moiré patterns formed by W and Te atoms separately. The W and Te patterns, assuming rigid layers, are shown in Figure 4a and Figure S11, respectively. This simplified view reveals that W atoms form 1D stripes while Te atoms form a triangular moiré pattern, although the Te layer should also reflect the rectangular superlattice structure, especially when their distributions in the vertical direction are considered. The overlapping of the six atomic layers in tWTe2 with a twist angle of ~5° forms a complex moiré pattern along the c axis as shown in Figure 4b. The triangular moiré pattern formed by Te atoms is difficult to identify in experimental STEM images, although STEM is a Zcontrast technique. However, the 1D pattern formed by W atoms is clearly observed, which looks consistent with the simulated moiré pattern formed by only W atoms. The HAADF-STEM image of tWTe2 confirms the strongly anisotropic moiré pattern forming a stripelike structure (owing to its rectangular cell), separated by a fixed interstripe distance of ~7.3 nm, close to the value reported by Wang et al. 15 (Figure 4a,c) Figure 4d suggests that the measured image agrees well with the simulation assuming rigid W layers; thus, we do not observe obvious reconstruction in tWTe2 at this twist angle of  $\sim 5^{\circ}$ .

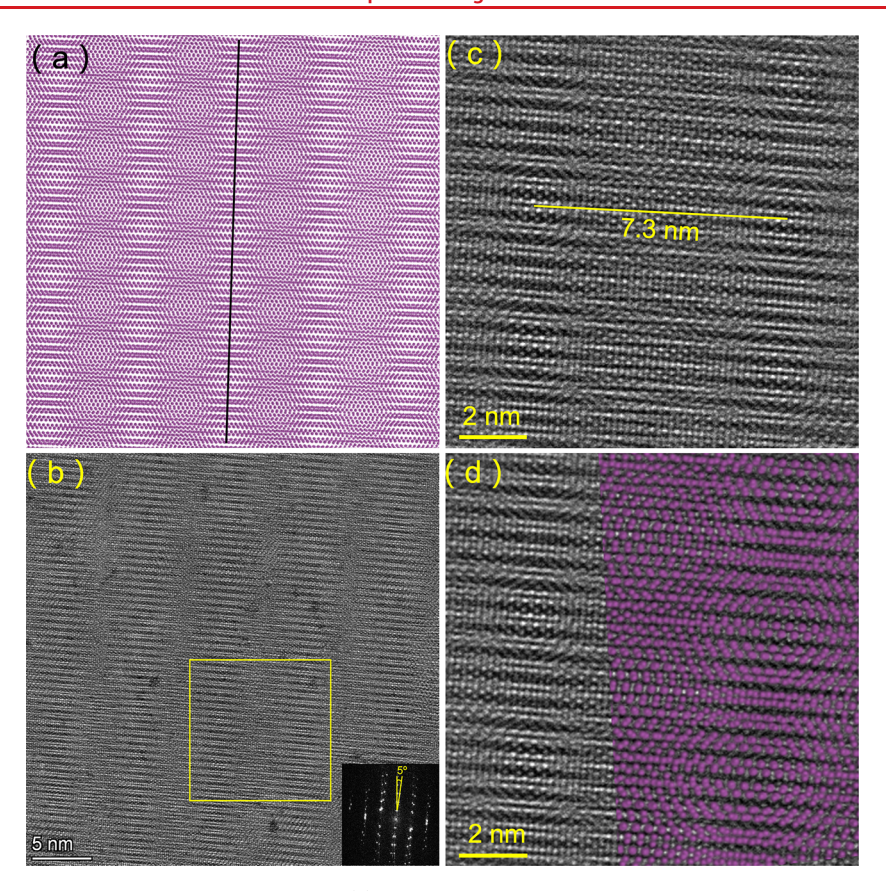


Figure 4. Moiré patterns of  $tWTe_2$  with a twist angle of  $\sim 5^\circ$ . (a) Simulated moiré pattern formed by W atoms. The direction of 1D W stripes is highlighted by a black line. (b) High-resolution STEM image of  $tWTe_2$  with a twist angle of  $\sim 5^\circ$ . The inset is the FFT pattern. (c) Enlarged STEM images labeled by yellow frame in (b). (d) Overlay of enlarged experimental STEM images with simulated W moiré pattern.

The assessment of reconstruction in the sample poses some uncertainty due to the limited resolution of the STEM images. Quantitative analysis regarding the extent of reconstruction becomes challenging under these circumstances. Our observations, based on the comparison between simulated and experimental STEM images, reveal no detectable reconstruction within the range of the standard deviation for atomicresolution STEM images (0.01 nm). Thus, a shift of atoms smaller than 0.01 nm may go unnoticed using this approach. Additionally, as noted above, the simulated images indicate the formation of 1D stripes by the W atoms and a triangular moiré pattern by the Te atoms. While the experimental STEM images clearly display the 1D pattern formed by the W atoms (in excellent agreement with the nonreconstructed simulated images), the triangular moiré pattern formed by the Te atoms remains unresolved in our experiments. Consequently, our discussion and conclusion regarding potential reconstruction primarily rely on the behavior of the W atoms. If there is any reconstruction associated with the Te atoms, it would remain undetected.

While we established that it seems highly unlikely that lattice reconstruction affects  $\sim\!5^\circ$  tWTe2, it is important to note that significant reconstruction is usually observed in samples with much smaller twist angles. We therefore analyzed another tWTe2 sample with a twist angle of  $\sim\!2^\circ$ , and the results can be found in Figure S12 in the SI. At this twist angle we could again not find any obvious signs of reconstruction; however, the picture is less clear than in the  $\sim\!5^\circ$  degree case. It remains possible that tWTe2 undergoes reconstruction at other angles. Still, thus far, moiré-induced properties have only been

experimentally detected in  $\sim 5^{\circ}$  tWTe<sub>2</sub>, which makes our confirmation of a lack of reconstruction in these samples relevant.

In principle, the imaging method described herein can be extended to other highly air-sensitive samples and twisted devices. We established an approach to obtain atomic-resolution images of tWTe<sub>2</sub> samples fabricated from mechanically exfoliated flakes. Future studies on tWTe<sub>2</sub> with different angles can help understand its potentially rich moiré physics.

In conclusion, we developed a methodology to prepare planview TEM samples from air-sensitive Scotch-tape-exfoliated monolayer and twisted-bilayer WTe2 samples. The procedure results in clean and suspended monolayer and twisted-bilayer WTe2 specimens. We established that the in-plane crystal structures of monolayer WTe2 are the same as its form in the bulk parent, confirmed by their identical in-plane d-spacings. We investigated the moiré patterns of tWTe2 with twist angles of approximately 5 and 2° and observed no noticeable lattice reconstruction. This observation is an important input for modeling of the atomic and electronic structures in this highly interesting material system. The direct visualization procedure described in this work deepens the understanding of the intrinsic microstructure of monolayer and twisted-bilayer WTe<sub>2</sub>, which is important for understanding and manipulating their quantum properties.

Nano Letters pubs.acs.org/NanoLett Letter

#### ASSOCIATED CONTENT

## **Supporting Information**

The Supporting Information is available free of charge at https://pubs.acs.org/doi/10.1021/acs.nanolett.3c01175.

Experimental descriptions of WTe2 bulk crystal growth, sample composition analysis, TEM sample preparation, and S/TEM, table of experimental and simulated dspacings of bulk Td-WTe2, figures of temperaturedependent resistivity of WTe2, SEM image and EDS spectrum of WTe2 single crystals, cross-sectional ARSTEM imaging and composition characterization of bulk WTe2 along the b axis, simulated selected area electron diffraction of bulk WTe2 along the b axis, optical microscope images of monolayer WTe2 on a Si/ SiO<sub>2</sub> wafer, optical microscope images of Si<sub>3</sub>N<sub>4</sub> TEM grids containing WTe2 samples, STEM images obtained at different accelerating voltages, degradation of monolayer Td-WTe2 under ambient conditions, AR-STEM images of few-layer WTe<sub>2</sub>, ARSTEM images of different regions containing large areas of flat WTe2 monolayer, simulated moiré pattern formed by Te atoms of tWTe2 with a twist angle of 5°, tWTe2 with a twist angle of ~2°, detailed discussion of structural characterization and composition analysis of bulk Td-WTe<sub>2</sub> crystals, instability and degradation of single- and fewlayer WTe2 nanosheets, and additional discussion of TEM/STEM investigation of monolayer WTe2 under 300 kV (PDF)

## AUTHOR INFORMATION

#### **Corresponding Authors**

Sanfeng Wu − Department of Physics, Princeton University, Princeton, New Jersey 08544, United States; oorcid.org/ 0000-0002-6227-6286; Email: sanfengw@princeton.edu

Leslie M. Schoop — Department of Chemistry, Princeton University, Princeton, New Jersey 08544, United States; orcid.org/0000-0003-3459-4241; Email: lschoop@princeton.edu

## **Authors**

Fang Yuan — Department of Chemistry, Princeton University, Princeton, New Jersey 08544, United States; orcid.org/0000-0001-7286-3233

Yanyu Jia — Department of Physics, Princeton University, Princeton, New Jersey 08544, United States; orcid.org/ 0000-0001-6061-8441

Guangming Cheng — Princeton Materials Institute, Princeton University, Princeton, New Jersey 08544, United States; orcid.org/0000-0001-5852-1341

Ratnadwip Singha — Department of Chemistry, Princeton University, Princeton, New Jersey 08544, United States; orcid.org/0000-0002-3155-2137

**Shiming Lei** – Department of Chemistry, Princeton University, Princeton, New Jersey 08544, United States

Nan Yao — Princeton Materials Institute, Princeton University, Princeton, New Jersey 08544, United States; orcid.org/0000-0002-4081-1495

Complete contact information is available at: https://pubs.acs.org/10.1021/acs.nanolett.3c01175

## **Author Contributions**

F.Y. and Y.J. contributed equally to this work.

#### **Notes**

The authors declare no competing financial interest.

#### ACKNOWLEDGMENTS

This work was supported by the Gordon and Betty Moore Foundation's EPIQS initiative through Grant GBMF9064, the David and Lucile Packard Foundation, the Princeton Catalysis Initiative (PCI), and the National Science Foundation (NSF)-Materials Research Science and Engineering Center (MRSEC; DMR-2011750). Y.J and S.W. acknowledge support from ONR through a Young Investigator Award (N00014-21-12804). S.W. and L.M.S. acknowledge the support from the Eric and Wendy Schmidt Transformative Technology Fund at Princeton. The authors acknowledge the sample characterization of the Imaging and Analysis Center (IAC) at Princeton University, partially supported by the Princeton Center for Complex Materials (PCCM) and the NSF-MRSEC program (MRSEC; DMR-2011750).

#### REFERENCES

- (1) Novoselov, K. S.; Mishchenko, A.; Carvalho, A.; Castro Neto, A. H. 2D materials and van der Waals heterostructures. *Science* **2016**, 353, aac9439.
- (2) Andrei, E. Y.; Efetov, D. K.; Jarillo-Herrero, P.; MacDonald, A. H.; Mak, K. F.; Senthil, T.; Tutuc, E.; Yazdani, A.; Young, A. F. The marvels of moiré materials. *Nature Reviews Materials* **2021**, *6*, 201–206
- (3) Mounet, N.; Gibertini, M.; Schwaller, P.; Campi, D.; Merkys, A.; Marrazzo, A.; Sohier, T.; Castelli, I. E.; Cepellotti, A.; Pizzi, G.; et al. Two-dimensional materials from high-throughput computational exfoliation of experimentally known compounds. *Nature Nanotechnol.* **2018**, *13*, 246–252.
- (4) Qian, X.; Liu, J.; Fu, L.; Li, J. Quantum Spin Hall Effect in Two-dimensional Transition Metal Dichalcogenides. *Science* **2014**, 346, 1344–1347.
- (5) Wu, S.; Fatemi, V.; Gibson, Q. D.; Watanabe, K.; Taniguchi, T.; Cava, R. J.; Jarillo-Herrero, P. Observation of The quantum Spin Hall Effect up to 100 K in a Monolayer Crystal. *Science* **2018**, *359*, 76–79.
- (6) Fei, Z.; Palomaki, T.; Wu, S.; Zhao, W.; Cai, X.; Sun, B.; Nguyen, P.; Finney, J.; Xu, X.; Cobden, D. H. Edge Conduction in Monolayer WTe, *Nat. Phys.* **2017**, *13*, 677–682.
- (7) Tang, S.; Zhang, C.; Wong, D.; Pedramrazi, Z.; Tsai, H.-Z.; Jia, C.; Moritz, B.; Claassen, M.; Ryu, H.; Kahn, S.; et al. Quantum Spin Hall State in Monolayer 1*T'*-WTe<sub>2</sub>. *Nat. Phys.* **2017**, *13*, 683–687.
- (8) Ali, M. N.; Xiong, J.; Flynn, S.; Tao, J.; Gibson, Q. D.; Schoop, L. M.; Liang, T.; Haldolaarachchige, N.; Hirschberger, M.; Ong, N. P.; et al. Large, Non-saturating Magnetoresistance in WTe<sub>2</sub>. *Nature* **2014**, *514*, 205–208.
- (9) Lee, C.-H.; Silva, E. C.; Calderin, L.; Nguyen, M. A. T.; Hollander, M. J.; Bersch, B.; Mallouk, T. E.; Robinson, J. A. Tungsten Ditelluride: a Layered Semimetal. *Sci. Rep.* **2015**, *5*, 1–8.
- (10) Jia, Y.; Wang, P.; Chiu, C.-L.; Song, Z.; Yu, G.; Jäck, B.; Lei, S.; Klemenz, S.; Cevallos, F. A.; Onyszczak, M.; et al. Evidence for a monolayer excitonic insulator. *Nat. Phys.* **2022**, *18*, 87–93.
- (11) Sun, B.; Zhao, W.; Palomaki, T.; Fei, Z.; Runburg, E.; Malinowski, P.; Huang, X.; Cenker, J.; Cui, Y.-T.; Chu, J.-H.; et al. Evidence for equilibrium exciton condensation in monolayer WTe2. *Nat. Phys.* **2022**, *18*, 94–99.
- (12) Wang, P.; Yu, G.; Jia, Y.; Onyszczak, M.; Cevallos, F. A.; Lei, S.; Klemenz, S.; Watanabe, K.; Taniguchi, T.; Cava, R. J.; et al. Landau Quantization and Highly Mobile Fermions in an Insulator. *Nature* **2021**, *589*, 225–229.
- (13) Fatemi, V.; Wu, S.; Cao, Y.; Bretheau, L.; Gibson, Q. D.; Watanabe, K.; Taniguchi, T.; Cava, R. J.; Jarillo-Herrero, P. Electrically tunable low-density superconductivity in a monolayer topological insulator. *Science* **2018**, *362*, 926–929.

Nano Letters pubs.acs.org/NanoLett Letter

- (14) Sajadi, E.; Palomaki, T.; Fei, Z.; Zhao, W.; Bement, P.; Olsen, C.; Luescher, S.; Xu, X.; Folk, J. A.; Cobden, D. H. Gate-induced superconductivity in a monolayer topological insulator. *Science* **2018**, 362, 922–925.
- (15) Wang, P.; Yu, G.; Kwan, Y. H.; Jia, Y.; Lei, S.; Klemenz, S.; Cevallos, F. A.; Singha, R.; Devakul, T.; Watanabe, K.; et al. One-dimensional Luttinger liquids in a two-dimensional moiré lattice. *Nature* **2022**, *605*, 57–62.
- (16) Lupke, F.; Waters, D.; Pham, A. D.; Yan, J.; Mandrus, D. G.; Ganesh, P.; Hunt, B. M. Quantum Spin Hall Edge States and Interlayer Coupling in Twisted Bilayer WTe<sub>2</sub>. *Nano Lett.* **2022**, 22, 5674–5680.
- (17) Yoo, H.; Engelke, R.; Carr, S.; Fang, S.; Zhang, K.; Cazeaux, P.; Sung, S. H.; Hovden, R.; Tsen, A. W.; Taniguchi, T.; et al. Atomic and electronic reconstruction at the van der Waals interface in twisted bilayer graphene. *Nature materials* **2019**, *18*, 448–453.
- (18) Kerelsky, A.; McGilly, L. J.; Kennes, D. M.; Xian, L.; Yankowitz, M.; Chen, S.; Watanabe, K.; Taniguchi, T.; Hone, J.; Dean, C.; et al. Maximized electron interactions at the magic angle in twisted bilayer graphene. *Nature* **2019**, *572*, 95–100.
- (19) Uri, A.; Grover, S.; Cao, Y.; Crosse, J. A.; Bagani, K.; Rodan-Legrain, D.; Myasoedov, Y.; Watanabe, K.; Taniguchi, T.; Moon, P.; et al. Mapping the Twist-angle Disorder and Landau Levels in Magicangle Graphene. *Nature* **2020**, *581*, 47–52.
- (20) Huder, L.; Artaud, A.; Le Quang, T.; De Laissardiere, G. T.; Jansen, A. G.; Lapertot, G.; Chapelier, C.; Renard, V. T. Electronic spectrum of twisted graphene layers under heterostrain. *Physical review letters* **2018**, 120, 156405.
- (21) Kazmierczak, N. P.; Van Winkle, M.; Ophus, C.; Bustillo, K. C.; Carr, S.; Brown, H. G.; Ciston, J.; Taniguchi, T.; Watanabe, K.; Bediako, D. K. Strain fields in twisted bilayer graphene. *Nature materials* **2021**, *20*, 956–963.
- (22) Weston, A.; Zou, Y.; Enaldiev, V.; Summerfield, A.; Clark, N.; Zólyomi, V.; Graham, A.; Yelgel, C.; Magorrian, S.; Zhou, M.; et al. Atomic reconstruction in twisted bilayers of transition metal dichalcogenides. *Nat. Nanotechnol.* **2020**, *15*, 592–597.
- (23) Van Winkle, M.; Craig, I. M.; Carr, S.; Dandu, M.; Bustillo, K. C.; Ciston, J.; Ophus, C.; Taniguchi, T.; Watanabe, K.; Raja, A., et al. Quantitative Imaging of Intrinsic and Extrinsic Strain in Transition Metal Dichalcogenide Moiré Bilayers. https://arxiv.org/abs/2212.07006 (accessed 2023-05-11), 2022.
- (24) Rosenberger, M. R.; Chuang, H.-J.; Phillips, M.; Oleshko, V. P.; McCreary, K. M.; Sivaram, S. V.; Hellberg, C. S.; Jonker, B. T. Twist angle-dependent atomic reconstruction and moiré patterns in transition metal dichalcogenide heterostructures. *ACS Nano* **2020**, *14*, 4550–4558.
- (25) Van Winkle, M.; Kazmierczak, N. P.; Ophus, C.; Bustillo, K. C.; Carr, S.; Brown, H. G.; Ciston, J.; Bediako, D. K. Direct Measurement of Atomic Reconstruction, Strain, and Disorder in Moiré Materials using 4D-STEM. *Microscopy and Microanalysis* **2022**, *28*, 1764–1766.
- (26) Naylor, C. H.; Parkin, W. M.; Gao, Z.; Kang, H.; Noyan, M.; Wexler, R. B.; Tan, L. Z.; Kim, Y.; Kehayias, C. E.; Streller, F.; et al. Large-area Synthesis of High-quality Monolayer 1T'-WTe<sub>2</sub> flakes. 2D Materials **2017**, 4, 021008.
- (27) Niu, K.; Weng, M.; Li, S.; Guo, Z.; Wang, G.; Han, M.; Pan, F.; Lin, J. Direct Visualization of Large-Scale Intrinsic Atomic Lattice Structure and Its Collective Anisotropy in Air-Sensitive Monolayer 1T'-WTe<sub>2</sub>. Advanced Science **2021**, *8*, 2101563.
- (28) Yu, P.; Lin, J.; Sun, L.; Le, Q. L.; Yu, X.; Gao, G.; Hsu, C.-H.; Wu, D.; Chang, T.-R.; Zeng, Q.; et al. Metal—Semiconductor Phase-Transition in  $WSe_{2(1-x)}Te_{2x}$  Monolayer. *Adv. Mater.* **2017**, 29, 1603991.
- (29) Jia, Y.; Yuan, F.; Cheng, G.; Tang, Y.; Yu, G.; Song, T.; Wang, P.; Singha, R.; Uzan, A. J.; Onyszczak, M.; Watanabe, K.; Taniguchi, T.; Yao, N.; Schoop, L. M.; Wu, S. Surface-Confined Two-Dimensional Crystal Growth on a Monolayer. http://arxiv.org/abs/2307.06477 (accessed 2023-07-14), 2023.
- (30) Obolonchik, V.; Vainer, L.; Yanaki, A. Chemical Stability of Tellurides of Subgroup VIa Transition Metals in Various Corrosive

Media. Soviet Powder Metallurgy and Metal Ceramics 1972, 11, 727–729.

(31) Wang, M.; Huang, M.; Luo, D.; Li, Y.; Choe, M.; Seong, W. K.; Kim, M.; Jin, S.; Wang, M.; Chatterjee, S.; et al. Single-crystal, Largearea, Fold-free Monolayer Graphene. *Nature* **2021**, *596*, 519–524.